ADVANCED FUNCTIONAL MATERIALS

High Mechanical Performance Composite Conductor: Multi-Walled Carbon Nanotube Sheet/Bismaleimide Nanocomposites

By *Qunfeng Cheng, Jianwen Bao, JinGyu Park, Zhiyong Liang,* Chuck Zhang,* and *Ben Wang*

Multi-walled carbon nanotube (MWNT)-sheet-reinforced bismaleimide (BMI) resin nanocomposites with high concentrations (~60 wt%) of aligned MWNTs are successfully fabricated. Applying simple mechanical stretching and prepregging (pre-resin impregnation) processes on initially randomly dispersed, commercially available sheets of millimeter-long MWNTs leads to substantial alignment enhancement, good dispersion, and high packing density of nanotubes in the resultant nanocomposites. The tensile strength and Young's modulus of the nanocomposites reaches 2 088 MPa and 169 GPa, respectively, which are very high experimental results and comparable to the state-of-the-art unidirectional IM7 carbon-fiber-reinforced composites for high-performance structural applications. The nanocomposites demonstrate unprecedentedly high electrical conductivity of 5 500 S cm^{-1} along the alignment direction. Such unique integration of high mechanical properties and electrical conductance opens the door for developing polymeric composite conductors and eventually structural composites with multifunctionalities. New fracture morphology and failure modes due to self-assembly and spreading of MWNT bundles are also observed.

1. Introduction

Many researchers predict carbon nanotubes (CNTs) to be the most promising candidate for the next generation of reinforcement materials, holding potential for replacing current reinforcement fiber materials, such as carbon fibers and Kevlar fibers, in the production of lightweight multifunctional/structural composites. Researchers hold this opinion due to CNTs' remarkable intrinsic mechanical,[1] electrical,[2] and thermal properties.[3] However, due to difficulties in fabricating high-quality macroscopic CNT-reinforced polymer composites with high nanotube loading (at least 20–60 wt% or more, using CNTs as reinforcements) and well aligned CNTs, nanocomposites have yet to meet or even come close to their expected performance. Therefore, composites made with CNTs continue to miss the mark for becoming comparable to the state-of-the-art aerospace-grade carbon fiber composites.

In contrast, high-performance fibrous materials, including both CNT/polymer composite fibers and neat CNT fibers, have recently been reported.[4] Due to their microscale sample size, good alignment, high nanotube concentration, and minimal defects,[5] CNT/polymer composite fibers and neat CNT fibers have exhibited excellent properties. Vigolo and Poulin[6,7] reported coagulation-spun single-walled nanotube (SWNT)/PVA composite fibers with a tensile strength of ~1.5 GPa, a Young's modulus of ~15 GPa, and electrical conductivity of 10 S cm^{-1} at room temperature. Dalton and Baughman[8] used a modified coagulation-spinning method to make super-tough SWNT/PVA composite fibers. These CNT composite fibers contain approximately 60 wt% SWNTs with a tensile strength of 1.8 GPa and Young's modulus of 80 GPa. Compared to CNT/polymer fiber, the strength of initial neat CNT fibers are relatively low due to an increased number of defects. Jiang and Fan[9] first developed a neat CNT yarn by dry-spinning super-aligned arrays of carbon nanotubes, which helped to transfer the outstanding properties of CNTs into macroscopic samples. The tensile strength and Young's modulus of these neat CNT fibers were about 600 MPa and 74 GPa, respectively.[10] Zhu, Ajayan, and co-workers[11] directly synthesized SWNT fiber with a tensile strength of 1.2 GPa and Young's modulus of 77 GPa, respectively. Zhang, Baughman, and Atkinson[12] introduced a dry stretching and twisting process for spinning CNT fibers, resulting in a tensile strength of 460 MPa and an electrical conductivity of 300 S cm^{-1} at room temperature. Ericson, Smalley, and co-workers[13] used a conventional spinning method to produce well-aligned SWNT fibers with a higher Young's modulus of 130 GPa and a tensile strength of 126 MPa. The electrical conductivity of these fibers was ~5 000 S cm^{-1}, with a thermal conductivity of 21 W m^{-1} K^{-1}. Li, Windle, and Kinloch[14] spun CNT fibers directly from the CVD synthesis zone of a furnace. The best electrical conductivity of their CNT

[*] Prof. Z. Liang, Dr. Q. Cheng, Dr. J. Bao, Dr. J. Park, Prof. C. Zhang, Prof. B. Wang
High-Performance Materials Institute (HPMI)
Florida State University
Tallahassee, FL 32310 (USA)
E-mail: liang@eng.fsu.edu

DOI: 10.1002/adfm.200900663

© 2009 WILEY-VCH Verlag GmbH & Co. KGaA, Weinheim

WILEY InterScience® DISCOVER SOMETHING GREAT

fibers was 8 300 S cm^{-1}, and the highest tensile strength reached 1.0 GPa. Recently, Koziol, Windle, and co-workers[15] combined direct spinning with a post-processing method to obtain high-performance CNT fibers. The optimum highest tensile strength of their CNT fiber was 8.8 GPa, and the Young's modulus was 357 GPa. The strength exceeded the mechanical properties of high-strength carbon-fiber materials, such as T1000G carbon fiber from Toray with a tensile strength of 6.37 GPa.[16] These results prove the potential of nanotubes in high-performance composite applications.

However, for real-world engineering applications of CNT-reinforced polymer composites, two major issues still exist: i) samples that reportedly showed high mechanical and electrical properties are small to be commercially applicable for real-world macroscopic structural applications and ii) to be adopted by industry, the manufacturing approach must be affordable and scalable in terms of production capacity and product size.

Herein, we describe the coupling of two otherwise simple processes—mechanical stretching and prepregging—where commercially available MWNT sheets and aerospace-grade BMI resin matrix were used to fabricate sizable CNT/BMI composites. Experimental results are presented and new fracture morphology and failure modes are discussed. The MWNT/BMI composites are unique in their high nanotube concentrations (60 wt%), good in-plane alignment, and well spreading of nanotube ropes as the result of mechanical stretching and prepregging. The resultant samples demonstrate high mechanical and electrical properties in macroscopic CNT/polymer composites.

2. Results and Discussion

2.1. Mechanical and Electrical Properties of Neat MWNT Sheets by Mechanical Stretching

Nanotube alignment is critical for realizing high mechanical performance. To date, two methods have been reported for nanotube alignment in neat CNT film materials: i) magnetic alignment,[17,18] which is used to align CNTs in a thin films or buckypapers by filtering CNT suspension in a high magnetic field, resulting in an alignment degree of SWNT characterized with Raman G-band intensity ratio of ~0.79 in buckypaper fabricated in a 26 Tesla field,[18] and ii) solid-state drawing,[9,10,12] which creates aligned nanotube thin films directly from synthesized CNT arrays. Although the CNT film drawn by solid-state drawing can reach macroscopic size, the creep resistance and mechanical properties of CNT film are low due to limited CNT length or small aspect ratio, and possible head-to-end connection of CNTs.[10] Currently, the height of a super-clean CNT array (vertically grown on a substrate) can only reach several hundred micrometers with relatively large nanotube diameters, which limit the aspect ratio of the CNTs. The major factor maintaining the integrity of these CNT films is primarily from van der Waals forces, along with some entanglement interactions among the CNTs. Such films therefore usually have poor in-plane mechanical properties and are difficult to stretch to improve alignment, again both due to a small aspect ratio in the range of 10 000. The randomly dispersed MWNT sheets manufactured by Nanocomp Technologies Inc. (Concord, NH) consist of millimeter-long and small-diameter (~3–8 nanometers) MWNTs with a range of 2–5 walls, providing a aspect ratio up to 100 000.[19] The sheets have substantial nanotube entanglements and possible interconnection through Nanocomp's proprietary floating catalyst synthesis and aero-gel condense method. The MWNT sheets can reach up to a meter long and are commercially available, which makes them practical for manufacturing bulk composites.

We used a simple mechanical-stretch method to align the MWNTs in the Nanocomp sheets. For example, for a 40%-stretched CNT sheet (i.e., the post-stretch sheet was 40% longer than the pre-stretch sheet), the degree of alignment of the CNT sheet can be dramatically improved, as shown in Figure 1A. To further understand and quantify the effects of the stretch ratio on the alignment degree, polarized Raman scattering tests were conducted and the alignment degree was calculated.[18,20] We measured polarized Raman intensity of the G-band as a function of angle between laser polarized direction and nanotube alignment direction or stretch axis. G-band Raman intensity shows the maximum if the polarization is parallel to the stretched axis ($\theta = 0$) and is at a minimum at the perpendicular direction ($\theta = 90$). Theoretical Raman intensity change simply follows $\cos^4 \theta$ versus nanotube orientation angle (θ). As described in Ref. [18], we simply use a two-dimensional distribution function to describe nanotube orientation distribution in the MWNT sheets. Then, we can obtain the best fitting curve of the Raman intensity versus orientation angle, as shown in Figure 1B. From the trend of the best fitting, we can predict the near perfect alignment (more than 95% nanotubes aligned along stretch direction) at an approximate 50% stretch ratio. However, the actual highest stretch ratio could only reach near 40%. Attempts to stretch such CNT sheets over 40% were not successful due to nanotube network breakage beyond what the current nanotube aspect ratio could handle.

Load carrying along the alignment direction showed improvements from the post-stretching samples. The mechanical properties of the neat (i.e., without polymer binders or resin) MWNT sheets of different stretch ratios were measured, as shown in Figure 1C. The tensile strength at break and Young's modulus of a randomly dispersed CNT sheet (the control sample) were approximately 205 MPa and 1.10 GPa, respectively. During stretching, the MWNTs self-assembled and aligned themselves along the load direction. The MWNT rope sizes increased and the packing density became higher compared to pre-stretched MWNT sheets. Along the alignment direction, the mechanical properties were significantly improved. The tensile strengths increased to 390 MPa, 508 MPa, and 668 MPa for the 30%, 35%, and 40% stretched samples, corresponding to 90%, 148% and 226% improvements, respectively. The post-stretch Young's modulus measurements along the alignment direction showed even more dramatic improvements, from 1.10 GPa for the randomly dispersed sheet (pre-stretch) to 11.93 GPa, 18.21 GPa, and 25.45 GPa, respectively, showing of 10-, 16-, and 22-fold improvements. Compared to other CNT sheets, such as buckypaper[21,22] or carbon nanotube films,[23] the MWNT sheets used in this study resulted in more entanglements that maintained the integrity of the nanotube networks due to a large aspect ratio. As a result, their mechanical properties and creep resistance were relatively high.

Since the mechanical properties of the neat MWNT sheets after stretching were dramatically increased along the alignment

WILEY InterScience DISCOVER SOMETHING GREAT
© 2009 WILEY-VCH Verlag GmbH & Co. KGaA, Weinheim

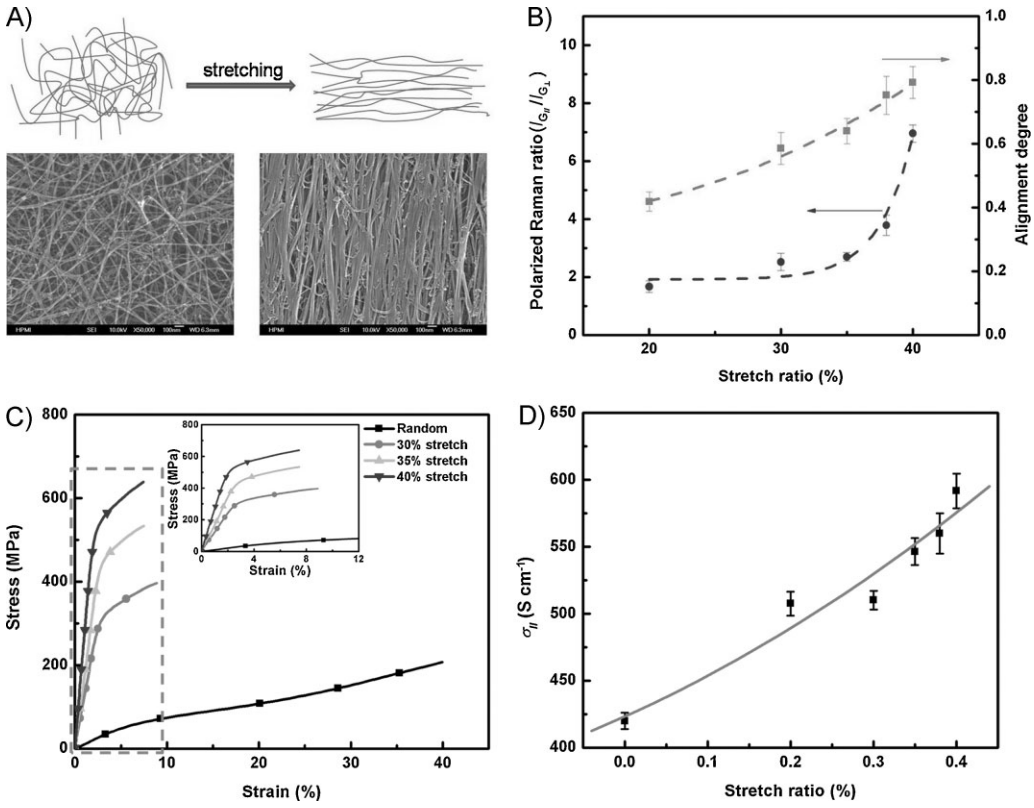

Figure 1. A) Schematic illustration of mechanical stretching to align nanotubes in the as-received random MWNT sheet. B) Effect of stretch ratio on degree of alignment. The G-band intensity ratio of the polarized Raman spectrum along parallel and perpendicular ($I_{G_{||}}$ and $I_{G_\perp}$)directions to the alignment (or stretching) direction indicates the extent of nanotube alignment. The relative alignment degree of a randomly dispersed CNT sheet is 0, whereas the perfect axial alignment degree is defined as 1[18]. Based on the ratio of $I_{G_{||}}/I_{G_\perp}$, the effect of the stretch ratio on the relative alignment degree was calculated. C) Typical tensile stress–strain curves of the neat MWNT sheets pre- and post-stretch. D) Effects of stretch ratio on electrical conductivity of the neat MWNT sheets parallel to the alignment (stretching) direction.

direction, the electrical conductivity of the sheets was expected to demonstrate improvements due to better alignment, denser packing, and better contacts among the MWNTs.[18,24] Figure 1D shows the electrical conductivity measurements of the neat MWNT sheets paralleled to the alignment direction. The electrical conductivity indeed became higher with the increased stretch ratio. Electrical conductivity ($\sigma_{//}$) paralleled to the alignment direction increased from 420 S cm^{-1} in the pre-stretched CNT sheets to 600 S cm^{-1} in the CNT sheet with a 40% stretch ratio. The electrical conductivity of the stretched sheets was not very high compared to the values of the nanotube fibers[14] previously discussed. This is because the neat MWNT sheets were still more porous.

Researchers have reported using buckypaper[25] or aligned CNT sheets[26] to reinforce polymer resin matrices to make composites. However, the mechanical properties of the composites were far below those of the state-of-the-art carbon fiber composites. Three reasons for this are speculated: i) the nanotube loading may be too low (less than 20 wt%); ii) a lack of adequate alignment;[27] iii) smaller aspect ratios of CNTs (less than 10 000) and hence poor load transfer between the matrix and CNTs when the composites are under loads.[27]

In this research, a three-prong approach was used to overcome the above technical hurdles. First, large-aspect-ratio, millimeter-long MWNTs were used. In addition, two effective manufacturing processes were adopted to realize high nanotube loading and good alignment in bulk composite samples. The high loading of CNTs in the polymer matrix was realized by using a prepregging process, which allowed us to achieve high nanotube loading and good resin/nanotube impregnation in each thin prepreg layer (10–20 μm) through resin B-stage compression and a precise control of the nanotube concentration in the resultant composites. A high degree of CNT alignment was realized with a conceptually simple mechanical stretching process. More detailed fabrication processes and mechanical test procedures are provided in the Supporting Information.

For this study, MWNT sheets were processed at three stretch ratios (30%, 35%, and 40%) for composite fabrication. The as-received (pre-stretched) randomly dispersed MWNT sheets were also to make composite samples (control samples). The composite samples had approximately 60 wt% nanotube weight fraction or loading.

2.2. Mechanical Properties and New Fracture Morphology of MWNT Sheet/BMI Nanocomposites

Figure 2A shows the typical uniaxial tensile stress–strain curves of the MWNT/BMI composites along the nanotube alignment

© 2009 WILEY-VCH Verlag GmbH & Co. KGaA, Weinheim

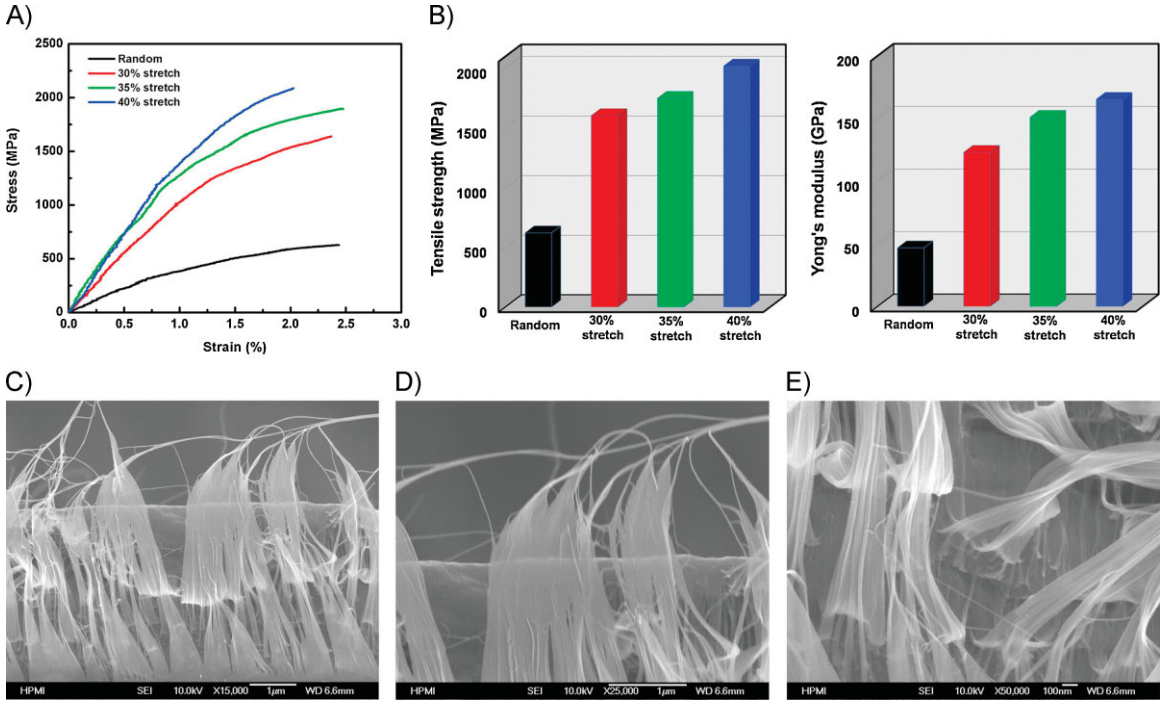

Figure 2. A) Typical tensile stress–strain curves of produced MWNT/BMI composites at different stretch ratios. B) Comparisons of tensile strength and Young's modulus measurements of the resultant composites at different stretch ratios. (C), (D), and (E) are scanning electron microscopy (SEM) images of typical fracture surface morphology of MWNT/BMI composites with a 40%-stretch ratio. Transparent thin films of MWNT/BMI indicates good spreading of MWNT ropes due to stretching and prepregging; stretched deformation of MWNT array along stress direction in the thin films implies good alignment and load transfer.

direction. Figure 2B summarizes the tensile strength and Young's modulus measurements of the samples. Figure 2A shows that the MWNT/BMI composites demonstrated a relatively large 2.0–2.5% failure strain compared to carbon-fiber-reinforced composites, typically in the range of 0.6–1.8%. The large tensile strains exceeded 2.0% because of CNTs' intrinsic flexibility, high failure elongation,[1] and high deformability of the MWNT networks in the sheets, as shown in Figure 1C. The tensile strength of the randomly dispersed MWNT/BMI composite (the control sample) was approximately 620 MPa, and the Young's modulus was 47 GPa. After stretching to improve alignment and nanotube packing, the mechanical properties dramatically increased. The tensile strength and Young's modulus of the 30%-stretched CNT/BMI composite were 1 600 MPa and 122 GPa, respectively. When the stretch ratio increased to 35%, the tensile strength and Young's modulus increased respectively to 1 800 MPa and 150 GPa. The tensile strength and Young's modulus of the 40%-stretched MWNT/BMI composite were as high as 2 088 MPa and 169 GPa, respectively.

Koziol, Windle, and co-workers[15] observed that the maximal alignment of nanotubes is crucial for realizing a high degree of contact between rigid neighboring CNTs and load-transfer efficiency. They successfully improved the mechanical strength of neat CNT fibers through enhanced densification and orientation in microscale fibrous material. In this study, the total number of nanotubes in the axial tensile direction dramatically increased (shown in Fig. 1B) with an increase in degree of alignment. Efficiency of both load carrying and transfer for the aligned nanotubes in the axial tensile direction was significantly enhanced, leading to dramatically higher mechanical properties. For example, the 40%-stretched sample had an alignment degree of the MWNTs along the axial direction of ~0.8 (seen in Fig. 1B), which means about 80% of the nanotubes were probably aligned along the stress direction to carry a load when the tensile stress was applied. Interfacial bonding between the CNTs and resin matrix was also an important factor. Ajayan and Tour[27] observed that the interactions between the CNTs and polymer chain are weak due to CNTs' atomically smooth surfaces. Covalent doping or functionalization can be used to improve the interfacial bonding.[28–30] However, chemical functionalization will usually lower the electrical and thermal conductivity of CNTs due to damaged nanotube structures hampering ballistic transport.[27] Such chemical functionalization could lead to either improved mechanical properties because of increased interfacial adhesion or reduced mechanical properties because of damaged CNT structures.

Figure 2C shows the fracture surface morphology of a 40%-stretched specimen after tensile tests. The MWNTs were peeled off as very thin and transparent films. BMI resin was suspected to coat on the nanotube bundle surface because high nanotube concentration and no bulk neat resin fractures were observed. This peeled off failure mode is not a result of individual MWNT sheets sliding to each other because the thickness of individual sheet is more than 10 μm. We can see the thickness of the peeled off thin films are much less than 100 nm (Fig. 2E). Many stretch deformations of the MWNT/BMI thin films were observed, indicating effective load transfer between the MWNTs and BMI

WILEY InterScience® DISCOVER SOMETHING GREAT
© 2009 WILEY-VCH Verlag GmbH & Co. KGaA, Weinheim

resin matrix in the composites. The evidences of MWNT slippage failure mode also can be seen in Figure 2C and D. The MWNTs were pulled out from the composites and became very stretched strips with obvious diameter change with sharp breaks at the end due to MWNT slippage within the bundles. Furthermore, although the resultant composites showed record-high mechanical properties, almost no broken nanotubes were seen—clear evidence that the full potential of CNTs' strength has yet to be completely realized. Further improvements in interfacial bonding and load transfer should be able to reach a much higher level of mechanical performance. The formed CNT/BMI thin films were transparent (seen in Fig. 2D), indicating that the thickness consisted of only a few layers of well-spread nanotubes. The spreading of nanotube bundles means the MWNT ropes morphed from original round and large-diameter shapes into flat thin-film shape during to mechanical stretching and prepregging processes. Such thin-film strips of nanotube assemblies can have much more nanotubes at the outmost layer to interact with other nanotube assemblies and resin matrix to achieve good load transfer.[31] The MWNTs were also well-aligned along the loading direction, which helped in realizing good load carrying. Such unique microstructures of the MWNT/BMI nanocomposites were results of the mechanical stretching and prepregging under pressure.

2.3 Thermal Mechanical Performance of MWNT Sheet/BMI Nanocomposites

Dynamic mechanical analysis (DMA) tests were conducted to confirm measured Young's modulus and measure glass transition temperature (T_g) values of MWNT/BMI samples. Figure 3A shows the comparison of the storage modulus measured. The storage modulus measurements of the composites were 55 GPa, 123 GPa, 147 GPa, and 172 GPa for the pre-stretched sample (the control sample), 30%-, 35%-, and 40%-stretched MWNT/BMI samples, respectively. The storage moduli of the CNT/BMI composites were consistent with the Young's modulus values in the tensile testing. The T_g readings (the peak temperature in the energy dissipation curves or tan δ curves) were 269.98 °C, 266.77 °C, 259.76 °C, and 256.70 °C for the control sample, 30%-, 35%-, and 40%-stretched MWNT/BMI composites, respectively (seen in Fig. 3B). It is important to note that the T_g values dropped 13.28°C from the random to 40%-stretched MWNT/BMI composites, which could mean that introducing high loading of CNTs reduced the crosslink density of the BMI resin. The reduction of the tan δ areas of the stretched MWNT composites could imply more molecular interactions between MWNTs and BMI due to more spreading of the MWNT ropes and large interface areas.

2.4 Mechanical-Property Comparison of MWNT/BMI Nanocomposites and Unidirectional Carbon-Fiber Composites

Figure 4A shows the comparisons of the mechanical properties between the MWNT/BMI composites with state-of-the-art aerospace-grade carbon fiber composites for structural applications.[32,33] We convert the MWNT wt% to vol% according to the ASTM D3171-99 method. In this study, the density of MWNT

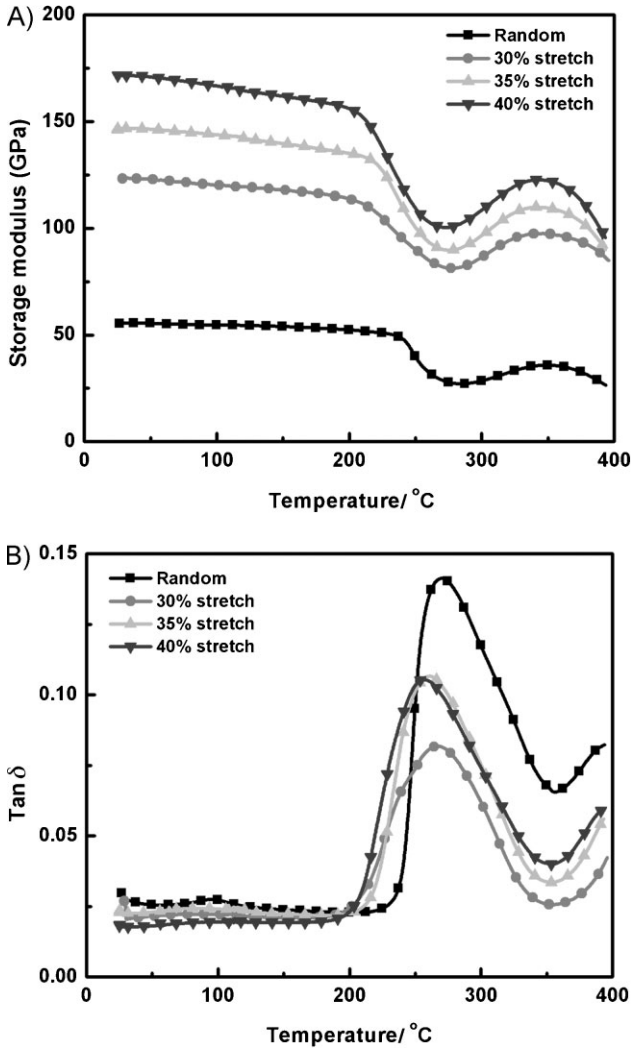

Figure 3. A) Comparisons of storage modulus and B) comparisons of tan δ curves of MWNT sheet/BMI nanocomposites.

and BMI resin are 1.8 g cm^{-3} and 1.25 g cm^{-3}, respectively. The measured density of the MWNT/BMI composite with 60 wt% MWNT loading is about 1.525 g cm^{-3}. The MWNT volume fraction calculated is about 50.83 vol%. For comparison with carbon-fiber composites, the mechanical properties of the MWNT/BMI composites were normalized to 60 vol% nanotube loading. The mechanical properties of the randomly dispersed MNWT sheet/BMI composite samples (the control samples) were close to those of carbon-fiber fabric composites. After alignment via mechanical stretching, the mechanical properties dramatically increased, and the property enhancement increased with improvements in the degree of alignment. When the stretch ratio reached 35%, the Young's modulus exceeded the current unidirectional (UD) carbon fiber composites. When the stretch ratio reached 40%, the tensile strength was comparable to that of Toray T700 or IM7 UD carbon fiber composites, and higher than that of Toray T300, AS4, and AS7 UD carbon fiber composites.[32,33] The 30%- and 40%-stretched samples proved to have a higher modulus than the UD carbon fiber composites.

© 2009 WILEY-VCH Verlag GmbH & Co. KGaA, Weinheim

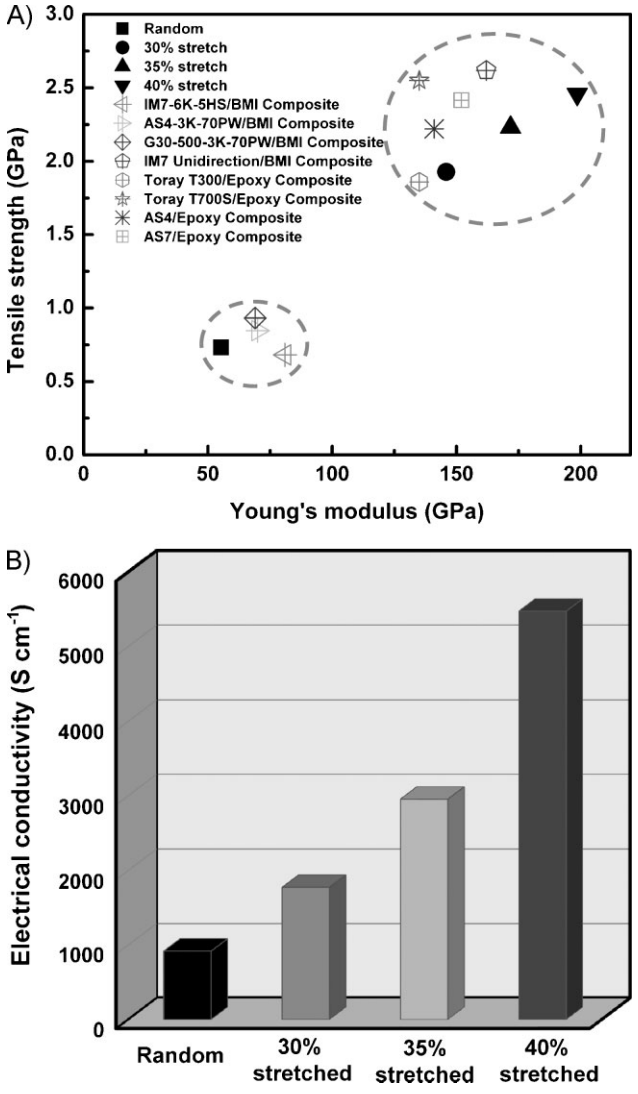

Figure 4. A) Mechanical property comparisons of produced MWNT/BMI composites and typical carbon fiber composites of aerospace structures. B) Electrical conductivity measurements parallel to the MWNT alignment direction in the composites with different stretch ratios.

2.5 Electrical Conductivity of MWNT/BMI Nanocomposites

Unprecedentedly high electrical conductivity was also realized in the stretched-MWNT/BMI composites. High electrical conductivity is desirable for multifunctional applications in nanotube composites.[31] The electrical conductivity of the MWNT/BMI composites was measured using the four-probe method, as summarized in Figure 4B. For the randomly dispersed control sample, the electrical conductivity was 915 S cm^{-1}, much higher than those of the reported nanotube composites,[26] as well as typical carbon fiber composites.[16,32,33] These high conductivity measurements were attributed to: i) high concentrations of MWNTs in the composite samples, ii) millimeter-long MWNTs without functionalization that preserved intrinsic electrical conductivity, and iii) dense packing of MWNTs leading to better contacts among nanotubes. For the stretched-MWNT/BMI composites, the electrical conductivity along the alignment direction of the CNTs ($\sigma_{//}$) was significantly higher than that of pre-stretched control samples. An increasing degree of alignment raised the electrical conductivity: 1,800 S cm^{-1} for the 30%-stretched specimen, to 3,000 S cm^{-1} for the 35%-stretched specimen, and 5,500 S cm^{-1} for the 40%-stretched specimen. The electrical conductivity ($\sigma_{//}$) of the 40%-stretched specimen was comparable to the aligned neat SWNT buckypaper.[18]

3. Conclusions

In summary, record-high mechanical and electrical properties of MWNT/BMI composites were realized. The coupling effects of millimeter-long MWNTs, mechanical stretching, and prepregging under high pressures led to high loading, good alignment, and enhanced load transfer. These factors are critical for mechanical property improvements. Additionally, successful dispersion of the nanotube ropes into spread-out extra-thin films led to better contacts among MWNTs, giving rise to effective load transfer and enhanced electrical conductivity. Integration of the high mechanical properties and unprecedented electrical conductance indicates these MWNT/BMI composites will lead to excellent materials for lightweight composite conductors for a wide range of multifunctional/structural applications.

4. Experimental

MWNT Sheet/BMI Nanocomposite Fabrication: The randomly dispersed MWNT sheets were supplied by Nanocomp Technologies Inc. The randomly dispersed sheets were mechanically stretched using a Shimadzu machine (AGS-J, Shimadzu Scientific Inc., Japan) to enhance nanotube alignment. The detailed stretching process is shown in Figure S1 of the Supporting Information. The stretching ratio of the MWNT sheets is calculated by Equation 1:

$$\Delta\% = \frac{L_2 - L_1}{L_1 - L_a - L_b} \times 100\% \quad (1)$$

Where L_1 and L_2 are the overall lengths of the MWNT sheet strips before and after stretching, L_a and L_b are the segment lengths held by the clamps (seen in Fig. S2, Supporting Information). The crosshead speed during stretching was 0.5 mm min^{-1} in all stretching experiments. The stretching deformation is irreversible. This is because the original nanotubes entanglements have been changed due to stretching force, and the nanotubes self-assembled into an aligned assembly due to van deer Waals interaction. Hence, there is no observed retraction after stretching. The final CNT sheets with different stretch ratios are shown in Figure S3 of the Supporting Information. We used both randomly dispersed (as-received) and stretched MWNT sheets to make MWNT/BMI resin matrix composites. Aerospace-grade BMI resin 5250-4 (Cytec. Inc) was chosen as the matrix resin. First, the MWNT sheets were impregnated with a BMI resin solution to make individual MWNT prepreg sheets with approximately 60 ± 2 wt% nanotube concentration or loading. The prepregging process is a solution impregnation process under pressure. The concentration of BMI resin in the solution needs to be adjusted to ensure low viscosity for facilitating impregnation. The residual solvent (acetone) was removed under 80 °C in the vacuum oven for 2 hours to make BMI/MWNT prepreg. Second, six layers of the MWNT sheet prepregs were stacked together and cured by the hot-press process with high pressure following the curing cycle: 375 °F (190.5 °C) for 4 hours plus 440 °F (226.7 °C) for 2 hours. The weight percentage of the nanotube was

WILEY InterScience DISCOVER SOMETHING GREAT
© 2009 WILEY-VCH Verlag GmbH & Co. KGaA, Weinheim

determined by the weights of total amount of MWNT sheets used during composite fabrication. The MWNT weight ratio in the final composite was controlled in the range of 60 ± 2 wt%.

In this study, the weight fractions of the random, 30%-, 35%-, and 40%-stretch MWNT composite samples were 60 w%, 61.7 wt%, 60.5 wt% and 61.7 wt%, respectively. The densities of MWNT and BMI resin were 1.8 g $cm^{-3}$and 1 25 g cm^{-3}, respectively. The measured density values of the composite samples are 1.525, 1.536, 1.530 and 1.536 g cm^{-3} respectively. Hence, the calculated void volume fractions are 0.367 vol%, 0.286 vol%, 0.227 vol%, 0.286 vol% for the samples, respectively. For comparison purpose, the void volume fraction requirement of conventional structural carbon fiber composites is less than 2 vol%. Hence, our samples have a good wetting between MWNTs and BMI resin, and low void volume content.

Characterization: Mechanical properties test were conducted using a Shimadzu machine with crosshead speed of 1 mm min^{-1} and gauge length of 20 mm under room temperature. The strain was recorded by Shimadzu non-contact video extensometer DVE-201. The specimens were cut into dog-bone shape with length of 35 mm and a working length of 20 mm and thickness of 60 μm according to ASTM D638. The typical tensile stress–strain curves of the MWNT sheets/BMI composite are shown in Figure S4, Figure S5, Figure S6, and Figure S7 of the Supporting Information. After the tensile tests, the fracture surface morphology of the specimens was coated with a gold layer and observed using an electronic scanning microscope (JEOL JSM-7401F USA, Inc.). Dynamic mechanical analysis (DMA) was performed on a DMA 800 machine (TA instrument Inc.) using the film mode with a constant frequency of 1 Hz from room temperature to 400 °C with a heating rate of 5 °C min^{-1}.

Acknowledgements

This research was supported by AFOSR and AFRL/RW (FA9550-05-1-0271, Investigation and Optimization of High-Performance Nanocomposites Produced with Nanotube Buckypaper Materials) and ONR STTR (NOOOI4-08-M-0348, High Loading Nanotube/BMI Composites) programs. The sponsorships and oversights of these programs by Dr. Charles Lee of the AFSOR and Dr. Ignacio Perez of the ONR are greatly appreciated. The authors also wish to thank Nanocomp Technologies Inc. for providing MWNT sheets. Supporting Information is available online from Wiley InterScience or from the authors.

Received: April 16, 2009
Revised: July 9, 2009
Published online: August 19, 2009

[1] M. F. Yu, O. Lourie, M. J. Dyer, K. Moloni, T. F. Kelly, R. S. Ruoff, *Science* **2000**, *287*, 637.
[2] A. Thess, R. Lee, P. Nikolaev, H. Dai, P. Petit, J. Robert, C. Xu, Y. H. Lee, S. G. Kim, A. G. Rinzler, D. T. Colbert, G. E. Scuseria, D. Tomanek, J. E. Fischer, R. E. Smalley, *Science* **1996**, *273*, 483.
[3] J. Hone, M. Whitney, C. Piskoti, A. Zettl, *Phys. Rev. B* **1999**, *59*, R2514.
[4] N. Behabtu, M. J. Green, M. Pasquali, *Nano Today* **2008**, *3*, 24.
[5] H. G. Chae, S. Kumar, *Science* **2008**, *319*, 908.
[6] B. Vigolo, A. Penicaud, C. Coulon, C. Sauder, R. Pailler, C. Journet, P. Bernier, P. Poulin, *Science* **2000**, *290*, 1331.
[7] B. Vigolo, P. Poulin, M. Lucas, P. Launois, P. Bernier, *Appl. Phys. Lett.* **2002**, *81*, 1210.
[8] A. B. Dalton, S. Collins, E. Munoz, J. M. Razal, V. H. Ebron, J. P. Ferraris, J. N. Coleman, B. G. Kim, R. H. Baughman, *Nature* **2003**, *423*, 703.
[9] K. Jiang, Q. Li, S. Fan, *Nature* **2002**, *419*, 801.
[10] X. B. Zhang, K. L. Jiang, C. Teng, P. Liu, L. Zhang, J. Kong, T. H. Zhang, Q. Q. Li, S. S. Fan, *Adv. Mater.* **2006**, *18*, 1505.
[11] H. W. Zhu, C. L. Xu, D. H. Wu, B. Q. Wei, R. Vajtai, P. M. Ajayan, *Science* **2002**, *296*, 884.
[12] M. Zhang, K. R. Atkinson, R. H. Baughman, *Science* **2004**, *306*, 1358.
[13] L. M. Ericson, H. Fan, H. Peng, V. A. Davis, W. Zhou, J. Sulpizio, Y. Wang, R. Booker, J. Vavro, C. Guthy, A. N. G. Parra-Vasquez, M. J. Kim, S. Ramesh, R. K. Saini, C. Kittrell, G. Lavin, H. Schmidt, W. W. Adams, W. E. Billups, M. Pasquali, W.-F. Hwang, R. H. Hauge, J. E. Fischer, R. E. Smalley, *Science* **2004**, *305*, 1447.
[14] Y. L. Li, I. A. Kinloch, A. H. Windle, *Science* **2004**, *304*, 276.
[15] K. Koziol, J. Vilatela, A. Moisala, M. Motta, P. Cunniff, M. Sennett, A. Windle, *Science* **2007**, *318*, 1892.
[16] Toray Carbon Fibers America, Inc. High Strength Carbon Fibers, http://www. toraycfa.com/pdfs/ T1000GData Sheet.pdf (last accessed February **2008**).
[17] D. A. Walters, M. J. Casavant, X. C. Qin, C. B. Huffman, P. J. Boul, L. M. Ericson, E. H. Haroz, M. J. O'Connell, K. Smith, D. T. Colbert, R. E. Smalley, *Chem. Phys. Lett.* **2001**, *338*, 14.
[18] J. E. Fischer, W. Zhou, J. Vavro, M. C. Llaguno, C. Guthy, R. Haggenmueller, M. J. Casavant, D. E. Walters, R. E. Smalley, *J. Appl. Phys.* **2003**, *93*, 2157.
[19] D. S. Lashmore, *Supercapacitors and Methods of Manufacturing Same*, US Patent No. 20080225464, **2008**.
[20] T. Liu, S. Kumar, *Chem. Phys. Lett.* **2003**, *378*, 257.
[21] A. G. Rinzler, J. Liu, H. Dai, P. Nikolaev, C. B. Huffman, F. J. Rodriguez-Macias, P. J. Boul, A. H. Lu, D. Heymann, D. T. Colbert, R. S. Lee, J. E. Fischer, A. M. Rao, P. C. Eklund, R. E. Smalley, *Appl. Phys. A-Mater.* **1998**, *67*, 29.
[22] M. Endo, H. Muramatsu, T. Hayashi, Y. A. Kim, M. Terrones, M. S. Dresselhaus, *Nature* **2005**, *433*, 476.
[23] M. Zhang, S. Fang, A. A. Zakhidov, S. B. Lee, A. E. Aliev, C. D. Williams, K. R. Atkinson, R. H. Baughman, *Science* **2005**, *309*, 1215.
[24] S. Pegel, P. Pötschke, T. Villmow, D. Stoyan, G. Heinrich, *Polymer* **2009**, *50*, 2123.
[25] Z. Wang, Z. Y. Liang, B. Wang, C. Zhang, L. Kramer, *Compos. Part. A-Appl. S* **2004**, *35*, 1225.
[26] Q. F. Cheng, J. P. Wang, K. L. Jiang, Q. Q. Li, S. S. Fan, *J. Mater. Res.* **2008**, *23*, 2975.
[27] P. M. Ajayan, J. M. Tour, *Nature* **2007**, *447*, 1066.
[28] L. Liu, A. H. Barber, S. Nuriel, H. D. Wagner, *Adv. Funct. Mater.* **2005**, *15*, 975.
[29] S. R. Wang, Z. Y. Liang, T. Liu, B. Wang, C. Zhang, *Nanotechnology* **2006**, *17*, 1551.
[30] Q. F. Cheng, J. W. Bao, X. P. Wang, R. Liang, C. Zhang, B. Wang, *SAMPE 09*, Baltimore, USA **2009**, Paper ID 201.
[31] J. Gou, Z. Liang, C. Zhang, B. Wang, *Compos. Part. B-Eng.* **2005**, *36*, 524–533.
[32] Toray Carbon Fibers America, Inc. Standard Modulus Carbon Fibers, http://www.toraycfa.com/pdfs/T300DataSheet.pdf (last accessed February **2008**).
[33] Hexcel Corporation, Carbon Fiber Data Sheets, ;1; http://www.hexcel.com/Products/Downloads/Carbon%20Fiber%20Data%20Sheets/ (last accessed February **2007**).

© 2009 WILEY-VCH Verlag GmbH & Co. KGaA, Weinheim